Supernovae constraints on models of dark energy reexamined

M. C. Bento,[1,*] O. Bertolami,[2,†] N. M. C. Santos,[1,‡] and A. A. Sen[1,§]
[1]*Departamento de Física and Centro de Física Teórica de Partículas, Instituto Superior Técnico, Avenida Rovisco Pais, 1049-001 Lisboa, Portugal*
[2]*Departamento de Física, Instituto Superior Técnico, Avenida Rovisco Pais, 1049-001 Lisboa, Portugal*
(Received 22 December 2004; published 3 March 2005)

We use the Type Ia Supernova gold sample data of Riess *et al* in order to constrain three models of dark energy. We study the Cardassian model, the Dvali-Turner gravity modified model, and the generalized Chaplygin gas model of dark energy–dark matter unification. In our best-fit analysis for these three dark energy proposals we consider the flat model and the nonflat model priors. We also discuss the degeneracy of the models with the XCDM model through the computation of the so-called jerk parameter.

DOI: 10.1103/PhysRevD.71.063501 PACS numbers: 98.80.–k, 98.80.Es

I. INTRODUCTION

The surprising discovery of the present late-time acceleration of the Universe [1] and the related fact that most of its energy is in the form of a mysterious dark energy is possibly one of the most puzzling issues of modern cosmology. Several scenarios have been put forward as a possible explanation. A positive cosmological constant, although the simplest candidate, is not particularly attractive given the extreme fine-tuning that is required to account for the observed accelerated expansion. This fact has led to models where the dark energy component varies with time, such as quintessence models.[1] In these models, the required negative pressure is achieved trough the dynamics of a single (light) scalar field [3] or, in some cases, two coupled scalar fields [4]. Despite some pleasing features, these models are not entirely satisfactory, since in order to achieve $\Omega_X \sim \Omega_m$ (where Ω_X and Ω_m are the dark energy and matter energy densities at present, respectively) some fine-tuning is required. Many other possibilities have been considered for the origin of this dark energy component such as a scalar field with a nonstandard kinetic term and k-essence models [5]; it is also possible to construct models which have $w_X = p/\rho < -1$, the so-called phantom energy models [6].

Recently, it has been proposed that the evidence for a dark energy component might be explained by a change in the equation of state of the background fluid with an exotic equation of state, the generalized Chaplygin gas (GCG) model [7–9]. The striking feature of this model is that it allows for a unification of dark energy and dark matter [9].

Another possible explanation for the accelerated expansion of the Universe could be the infrared modification of gravity one should expect from, for instance, extra dimensional physics, which would lead to a modification of the effective Friedmann equation at late times [10–12]. An interesting variation of this proposal has been suggested by Dvali and Turner [10] (hereafter referred to as DT model). Another possibility, also originally motivated by extra-dimensions physics, is the modification of the Friedmann equation by the introduction of an additional nonlinear term proportional to ρ^n, the so-called Cardassian model [13].

Currently type Ia supernovae (SNe Ia) observations provide the most direct way to probe the dark energy component at low to medium redshifts. This is due to the fact that supernova data allows for a direct measurement of the luminosity distance, which is directly related to the expansion law of the Universe which, in turn, is the physical quantity that is directly related with dark energy or that is modified by extra dimensional physics. This approach has been explored by various groups in order to obtain insight into the nature of dark energy. Indeed, recently supernova data with 194 data points has been analyzed [14] and it was shown that it yields relevant constraints on some cosmological parameters. In particular, it is possible to conclude that, when one considers the full supernova data set, the decelerating model is ruled out with a significant confidence level. It is also shown that one can measure the current value of the dark energy equation of state with higher accuracy and the data prefers the phantom kind of equation of state, $w_X < -1$. Furthermore, the most significant result of that analysis is that, without a flat prior, that supernova data does not favor a flat ΛCDM model at least up to a 68% confidence level, which is consistent with other cosmological observations. In what concerns the equation of state of the dark energy component, it has been shown in Ref. [15], using the same set of supernovae data, that the best-fit equation of state of dark energy evolves rapidly from $w_X \simeq 0$ in the past to $w_X \lesssim -1$ in the present, which suggests that a time varying dark energy is better fitted with the data than the ΛCDM model. This

*Electronic address: bento@sirius.ist.utl.pt
†Electronic address: orfeu@cosmos.ist.utl.pt
‡Electronic address: ncsantos@cftp.ist.utl.pt
§Electronic address: anjan@cftp.ist.utl.pt
[1]An evolving vacuum energy was discussed somewhat earlier, see, e.g., Refs. [2].

result is also robust to changes of Ω_m and remains valid for the interval $0.1 \leq \Omega_m \leq 0.5$. Supernova data has also been used in the context of different cosmological models for dark energy [16–21]. In this paper, we analyze the Cardassian, the DT, and the GCG models in light of the Riess *et al.* SNe Ia compilation of data [22]. We consider both flat and nonflat priors.

Notice, however, that our analysis is restricted to the very late history of the Universe and does not address dark energy effects on the cosmic microwave background fluctuations or on structure formation.

This paper is organized as follows. In Sec. II we describe our best-fit analysis of SNe Ia data that will be employed as methodology to constrain the dark energy models we have studied, namely, the Cardassian, DT, and GCG models. In Sec. III we consider the best-fit analysis to constrain the Cardassian dark energy model. In Sec. IV, we discuss the DT model and in Sec. V the dark energy–dark matter unification GCG model. Section VI is devoted to the discussion of the degeneracy of the discussed models with the XCDM model through the introduction of the so-called jerk parameter. In Sec. VII we present our conclusions.

II. OBSERVATIONAL CONSTRAINTS FROM SUPERNOVAE DATA

The observations of supernovae measure essentially the apparent magnitude m, which is related to the luminosity distance d_L by

$$m(z) = \mathcal{M} + 5\log_{10} D_L(z), \tag{1}$$

where

$$D_L(z) \equiv \frac{H_0}{c} d_L(z), \tag{2}$$

is the dimensionless luminosity distance and

$$d_L(z) = (1+z) d_M(z), \tag{3}$$

with $d_M(z)$ being the comoving distance given by

$$d_M(z) = c \int_0^z \frac{1}{H(z')} dz'. \tag{4}$$

Also,

$$\mathcal{M} = M + 5\log_{10}\left(\frac{c/H_0}{1\text{Mpc}}\right) + 25, \tag{5}$$

where M is the absolute magnitude which is believed to be constant for all supernovae of type Ia.

For our analysis, we consider the two sets of supernovae data recently compiled by Riess *et al.* [22]. The first set contains 143 points from previously published data that were taken from the 230 Tonry *et al.* [23] data along with the 23 points from Barris *et al.* [24]. They have discarded various points where the classification of the supernovae was not certain or the photometry was incomplete, increasing the reliability of the sample. The second set contains the 143 points from the first one plus 14 points discovered recently using the Hubble Space Telescope (HST)[22] and is named as 'gold' sample, following Riess *et al.*. We will name the first sample as gold without HST. The main difference between the two samples is that the full gold sample also covers higher redshifts ($1 < z < 1.6$).

The data points in these samples are given in terms of the distance modulus

$$\mu_{\text{obs}}(z) \equiv m(z) - M_{\text{obs}}(z), \tag{6}$$

and the errors $\sigma_{\mu_{\text{obs}}}(z)$ already quoted take into account the effects of peculiar motions.

The χ^2 is calculated from

$$\chi^2 = \sum_{i=1}^{n}\left[\frac{\mu_{\text{obs}}(z_i) - \mathcal{M}' - 5\log_{10} D_{L\text{th}}(z_i; c_\alpha)}{\sigma_{\mu_{\text{obs}}}(z_i)}\right]^2, \tag{7}$$

where $\mathcal{M}' = \mathcal{M} - M_{\text{obs}}$ is a free parameter and $D_{L\text{th}}(z; c_\alpha)$ is the theoretical prediction for the dimensionless luminosity distance of a supernova at a particular distance, for a given model with parameters c_α. It can be computed for each model from the Friedmann expansion law [cf. Equations (9), (14), and (17) below] combined with Eqs. (2)–(4).

In the following, we will consider the three models referred to in the Introduction and perform a best-fit analysis with the minimization of the χ^2, Eq. (7), with respect to $\mathcal{M}'$, Ω_m, Ω_k, and the respective model parameter(s), using a MINUIT [25] based code.

The allowed variation range of the parameters is presented in Table I. $\mathcal{M}'$ is a model independent parameter and hence its best-fit value should not depend on the specific model. We found that the best-fit value for $\mathcal{M}'$ for all the models considered here is 43.3, which is consistent with the one obtained in [14]. Hence, we have also used this value for $\mathcal{M}'$ throughout our analysis. We have also checked that the result does not change if we marginalize over $\mathcal{M}'$.

In what follows we shall present a description of the models that are considered in this analysis and perform the best-fit study considering flat and nonflat priors. Our results are summarized in Table II.

TABLE I. Parameter range for the best-fit analysis.

Parameters	Range
Ω_m or A_s	$]0, 1[$
Ω_k	$]-1, 1[$
$\mathcal{M}'$	$[41, 45]$
Cardassian: n	$[-30, 2/3]$
DT: β	$[-60, 1]$
GCG: α	$[0, 10]$

TABLE II. Best-fit parameters for the Cardassian, DT, and GCG models, for the two data samples of Riess *et al.*, considering flat and nonflat priors. The best-fit value used for $\mathcal{M}'$ is 43.3.

	Data Sample	Ω_m or A_s	Model parameter	Ω_k	χ^2
Cardassian model					
Flat	Gold w/o HST	0.53	−2.0	···	154.6
Prior	Gold	0.49	−1.4	···	173.7
Non-Flat	Gold w/o HST	0.97	−0.93	−0.75	154.4
Prior	Gold	0.21	−3.1	0.47	173.2
DT model					
Flat	Gold w/o HST	0.55	−60.0	···	155.4
Prior	Gold	0.51	−19.2	···	174.7
Non-Flat	Gold w/o HST	1.0	−15.6	−0.71	155.0
Prior	Gold	0.24	−60.0	0.43	174.0
GCG model					
Flat	Gold w/o HST	0.98	6.2	···	155.0
Prior	Gold	0.93	2.8	···	174.2
Non-Flat	Gold w/o HST	0.73	1.3	−1.0	154.2
Prior	Gold	0.97	4.0	0.02	174.5

III. CARDASSIAN MODEL

We first consider the Cardassian model [13], which justifies the late-time accelerating Universe by invoking an additional term in the Friedmann equation proportional to ρ^n. In this model, the Universe is composed only of radiation and matter (including baryon and cold dark matter) and the increasing expansion rate is given by

$$H^2 = \frac{8\pi}{3M_{\rm Pl}^2}(\rho + b\rho^n) - \frac{k}{a^2} \tag{8}$$

where $M_{\rm Pl} = 1.22 \times 10^{19}$ GeV is the 4-dimensional Planck mass, b and n are constants, and we have added a curvature term to the original Cardassian model. At present, the Universe is matter dominated, i.e. $\rho_m \gg \rho_{\rm rad}$, hence $\rho \approx \rho_m$. The new term dominates only recently, at about $z \sim 1$, hence in order to get the recent acceleration in the expansion rate, $n < 2/3$ is required.

The theoretical motivation for the Cardassian term is fairly speculative. It can be argued that its origin may arise as a consequence of embedding our (3 + 1)-dimensional brane universe in extra-dimensions [26], or from some unknown interactions between matter particles [27].

In a matter dominated universe, Eq. (8) can be rewritten as

$$\left(\frac{H}{H_0}\right)^2 = \Omega_m(1+z)^3 + \Omega_k(1+z)^2 + (1-\Omega_m-\Omega_k)(1+z)^{3n}, \tag{9}$$

where H_0 is the present day value of the Hubble constant and $\Omega_k = -\frac{k}{a_0^2H_0^2}$ is the present curvature parameter. Notice

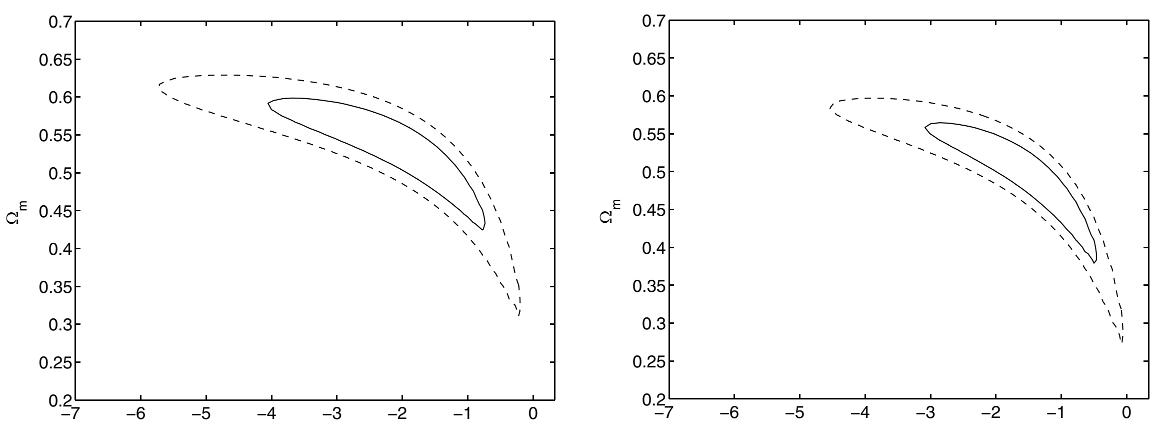

FIG. 1. Confidence contours in the $\Omega_m - n$ parameter space for the flat Cardassian model. The solid and dashed lines represent the 68% and 95% confidence regions, respectively; in the left panel are shown the results for the gold sample without the HST SNe Ia, whereas in the right panel, the full gold sample is taken into account.

that the only parameter of the model is n and that the case $n = 0$ corresponds to the ΛCDM model.

The best-fit results for this model, for the two data samples we are considering, and taking into account flat and nonflat priors, are summarized in Table II.

For the flat case, we have only two parameters and the best-fitting results we get are $\{\Omega_m, n\} = \{0.53, -2.0\}$, without HST, and $\{\Omega_m, n\} = \{0.49, -1.4\}$, with HST SNe Ia. In Fig. 1 we show the 68% and 95% confidence contour plots. These results are consistent with those obtained in previous works by Gong and Duan [18], Zhu *et al.* [19], and Sen and Sen [21] for other data sets. Hence, we see that the case $n = 0$, which corresponds to the ΛCDM model, is excluded at a 95% confidence level by both samples, even though the HST sample favors slightly larger values of n.

If we relax the flat prior and consider the curvature, we find that the best-fit analysis reveals that the gold sample without HST data favors a negative curvature around

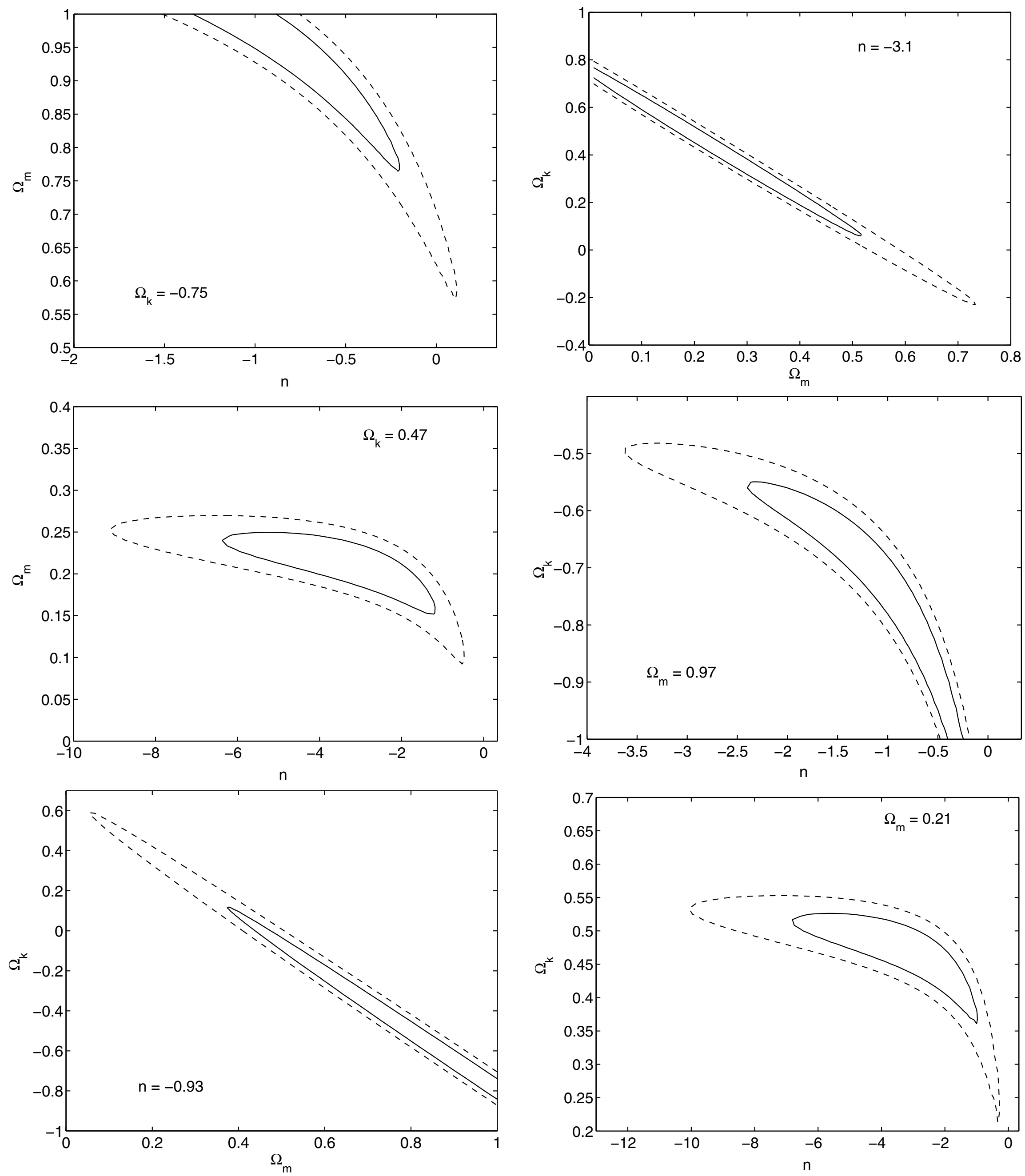

FIG. 2. Confidence contours in the $\Omega_m - n$, $\Omega_k - \Omega_m$, and $\Omega_k - n$ parameter space for the nonflat Cardassian model. As in Fig. 1, the solid and dashed lines represent the 68% and 95% confidence regions, respectively; in the left panel the golden sample is used without HST SNe Ia, whereas in the right one the full gold sample is taken into account.

$\Omega_k = -0.75$, with a significant matter component, $\Omega_m = 0.97$, even though the 68% confidence contour region (see Fig. 2) is consistent with curvatures in the range $[-1, 0.1]$ and matter density in the range $[0.38, 1]$; for the model parameter we find that it lies in the range $[-2.4, -0.2]$ with central value $n = -0.93$. From the 95% confidence contour, meaningful bounds can be still obtained for the model parameter: n must lie in the range $[-3.6, 0.1]$, hence not excluding the ΛCDM model. Values for Ω_k and, mainly, Ω_m cannot be significantly constrained.

Clearly the HST data brings the amount of matter to lower values, but pushes curvature to positive values and the model parameters for values that are smaller than the ones obtained with gold without HST data. We find that the best-fitting value for the curvature is significantly positive $\Omega_k = 0.47$ and $\Omega_m = 0.21$; for the model parameter we obtain as best-fit value -3.1. Moreover, the $n = 0$ case is excluded with a 95% confidence level. The contour plots are presented in Fig. 2.

IV. DVALI-TURNER MODEL

The second model we will consider is the one proposed by Dvali and Turner [10], where the Friedmann equation is modified by the addition of the term $H^\beta/r_c^{2-\beta}$, which can arise in theories with extra dimensions [11]; r_c is a crossover scale which sets the scale beyond which the laws of the 4-dimensional gravity breakdown and become 5-dimensional. In this case, in contrast with theories with infinite volume extra dimensions, the laws of gravity are modified in the far infrared and the cosmological evolution gets modified at late times; the short distance gravitational dynamics is very close to that of the 4-dimensional Einstein gravity, hence the early times cosmological evolution is very close to the Friedmann-Robertson-Walker picture.

As a motivation for this type of modification of gravity, consider the model with a single extra dimension [11,12], with the effective low-energy action given by

$$S = \frac{M_{\rm Pl}^2}{r_c}\int d^4x dy \sqrt{g^{(5)}}\mathcal{R} + \int d^4x\sqrt{g}(M_{\rm Pl}^2 R + \mathcal{L}_{\rm SM}), \tag{10}$$

where y is the extra spatial coordinate, $g^{(5)}$ is the trace of the 5-dimensional metric $g_{AB}^{(5)}$ $(A, B = 0, 1, 2, ..., 4)$, g the trace of the 4-dimensional metric induced in the brane, $g_{\mu\nu}(x) \equiv g_{\mu\nu}^{(5)}(x, y = 0)$. The first term in the action is the bulk 5-dimensional Einstein action, where $\mathcal{R}$ is the 5-dimensional Ricci scalar, and the second one is the 4-dimensional Einstein term, localized on the brane (at $y = 0$), where R is the 4-dimensional Ricci scalar and $\mathcal{L}_{\rm SM}$ is the Lagrangian of the fields in the standard model. For the maximally-symmetric FRW ansatz, $ds_5^2 = f(y, H)ds_4^2 - dy^2$, where ds_4^2 is the 4-dimensional maximally-symmetric metric, one gets the modified Friedmann equation on the brane

$$H^2 \pm \frac{H}{r_c} = \frac{8\pi}{3M_{\rm Pl}^2}\rho, \tag{11}$$

where ρ is the total energy density in the brane.

Inspired in this construction, Dvali and Turner considered a more generic (and radical) modification of the Friedmann equation [10]

$$H^2 - \frac{H^\beta}{r_c^{2-\beta}} = \frac{8\pi}{3M_{\rm Pl}^2}\rho - \frac{k}{a^2}, \tag{12}$$

where we have also introduced the curvature term in the brane. The crossover scale r_c is fixed in order to eliminate the need for dark energy,

$$r_c = H_0^{-1}(1 - \Omega_m - \Omega_k)^{1/(\beta-2)}, \tag{13}$$

where we assume again that the Universe is matter dominated. The Friedmann expansion law can then be written as

$$\left(\frac{H}{H_0}\right)^2 = \Omega_m(1+z)^3 + (1 - \Omega_m - \Omega_k)\left(\frac{H}{H_0}\right)^\beta + \Omega_k(1+z)^2. \tag{14}$$

Notice that β is the only parameter of the model: for $\beta = 0$ the new term behaves like a cosmological constant, and for $\beta = 2$ it corresponds to a "renormalization" of the Friedmann equation. Note also that the case $\beta = 1$ corresponds to the model in Eq. (11), hereafter called the Dvali-Gabadadze-Porrati (DGP) model [11]. The successful predictions of the big bang nucleosynthesis impose a limit on β, namely, $\beta \leq 1.95$; a more stringent bound follows from requiring that the new term does not interfere with the formation of large-scale structure: $\beta \leq 1$. Moreover, it can be shown that, in the recent past ($10^4 > z \gg 1$), this correction behaves like dark energy with equation of state $w_{\rm eff} = -1 + \beta/2$, and $w = -1$ in the distant future and, moreover, it can mimic $w < -1$ without violating the weak-energy condition [10].

For the flat DT model, the best-fitting parameters are $\{\Omega_m, \beta\} = \{0.55, -60.0\}$ without HST and $\{\Omega_m, \beta\} = \{0.51, -19.2\}$ with HST supernovae, as is summarized in Table II. From Fig. 3, where the 68% and 95% confidence contour plots are shown, it is clear that β is very weakly constrained by both supernovae data sets, and can become arbitrarily large and negative. Moreover, the cosmological constant, corresponding to $\beta = 0$, seems to be disfavored; also $\beta = 1$, the DGP model, is strongly disfavored. These results are consistent with those of Elgaroy *et al.* [20] obtained with another data set.

If we fix $\beta = 1$ (DGP model), and allow only Ω_m to vary, the best-fit values are $\Omega_m = 0.17$ and $\Omega_m = 0.16$ for the gold sample and gold sample without HST SNe Ia, respectively, which are consistent with the results of Gong and Duan [18].

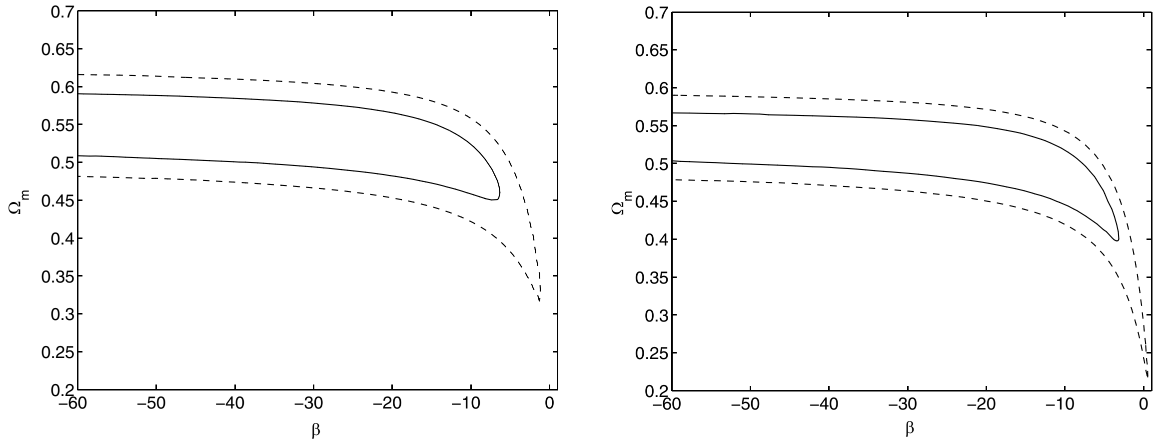

FIG. 3. Confidence contours in the $\Omega_m - \beta$ parameter space for the flat DT model. The solid and dashed lines represent the 68% and 95% confidence regions, respectively; in the left panel are shown the results for the gold sample without the HST SNe Ia, whereas in the right the full gold sample is taken into account.

Now, if we relax the flat prior, we find that $\{\Omega_k, \beta\} = \{-0.71, -15.6\}$ are the best-fit values for the gold sample without HST SNe Ia (Table II); the best-fit value for Ω_m is in the end of the variation range we considered for this parameter, $\Omega_m = 1$. As we can see from the contour plots shown in Fig. 4, Ω_m cannot be constrained at 95% confidence level, however the 68% confidence contours show that data prefer $\Omega_m > 0.25$. In what concerns β, it can

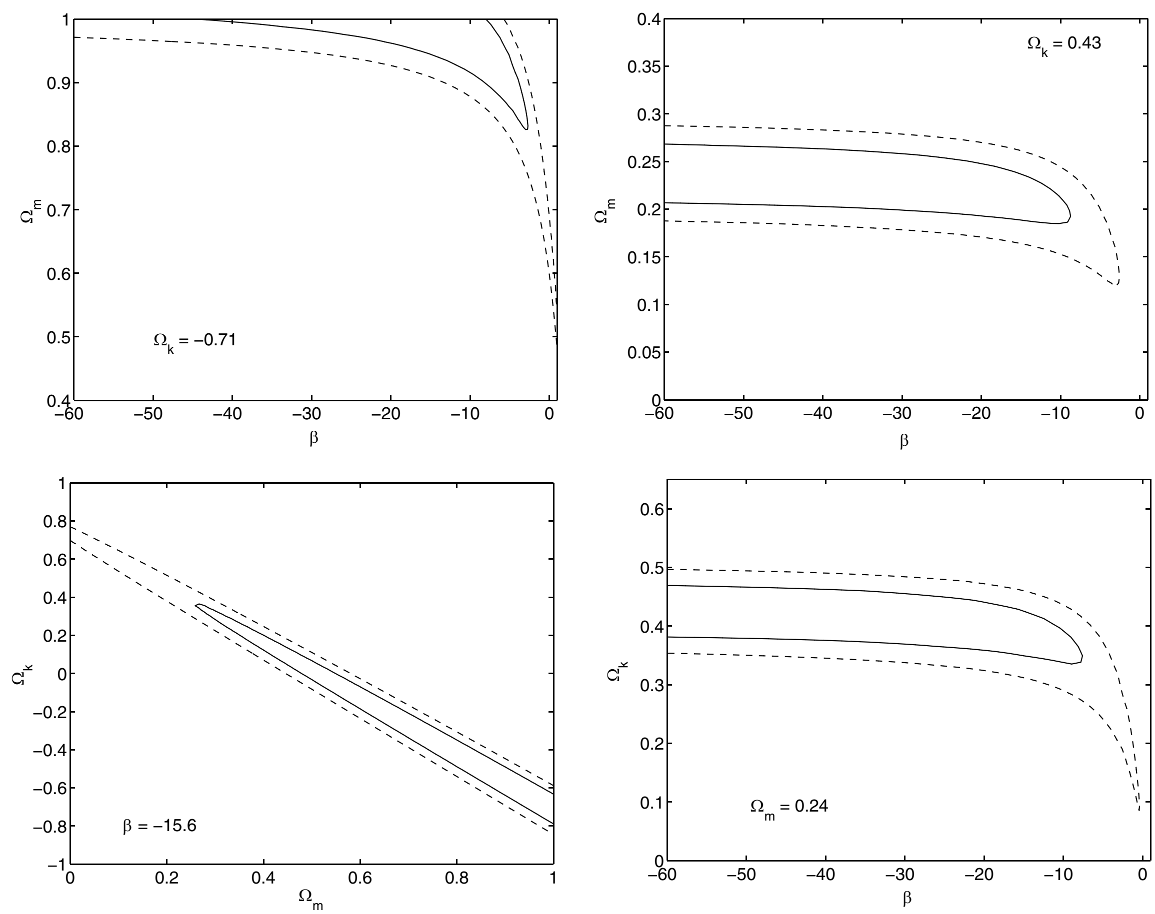

FIG. 4. Confidence contours in the $\Omega_m - \beta$ and $\Omega_k - \Omega_m$ parameter space for the nonflat DT model using the gold sample without HST SNe Ia (left panel) and in the $\Omega_m - \beta$ and $\Omega_k - \beta$ plane using the full gold sample (right panel). As in Fig. 3, the solid and dashed lines represent the 68% and 95% confidence regions, respectively.

become arbitrarily large and negative, if we allow Ω_m to be large. Moreover, both ΛCDM and DGP models are disfavored with 68% confidence.

Once more the HST data brings the amount of matter to lower values and pushes curvature to positive values. The best-fit results are $\{\Omega_m, \Omega_k, \beta\} = \{0.24, 0.43, -60, 0\}$. Also in this case both ΛCDM and DGP models are disfavored.

V. GENERALIZED CHAPLYGIN GAS MODEL

Finally, we consider the generalized Chaplygin gas model, which is characterized by the equation of state

$$p_{ch} = -\frac{A}{\rho_{ch}^{\alpha}}, \tag{15}$$

where A and α are positive constants. For $\alpha = 1$, the equation of state is reduced to the Chaplygin gas scenario [7].

Integrating the energy conservation equation with the equation of state (15), one gets [9]

$$\rho_{ch} = \rho_{ch0}\left[A_s + \frac{(1 - A_s)}{a^{3(1+\alpha)}}\right]^{1/(1+\alpha)}, \tag{16}$$

where ρ_{ch0} is the present energy density of GCG and $A_s \equiv A/\rho_{ch0}^{(1+\alpha)}$. One of the most striking features of this expression is that the energy density of this GCG, ρ_{ch}, interpolates between a dust dominated phase, $\rho_{ch} \propto a^{-3}$, in the past and a de-Sitter phase, $\rho_{ch} = -p_{ch}$, at late times. This property makes the GCG model an interesting candidate for the unification of dark matter and dark energy. Moreover, one can see from the above equation that A_s must lie in the range $0 \leq A_s \leq 1$: for $A_s = 0$, GCG behaves always as matter whereas for $A_s = 1$, it behaves always as a cosmological constant. We should point out, however, that if we want to unify dark matter and dark energy, one has to exclude these two possibilities resulting the range for A_s as $0 < A_s < 1$. Notice also that $\alpha = 0$ corresponds to the ΛCDM model.

The Friedmann equation for a nonflat unified GCG model in general is given by

$$\left(\frac{H}{H_0}\right)^2 = (1 - \Omega_k)[A_s + (1 - A_s)(1 + z)^{3(1+\alpha)}]^{1/(1+\alpha)} + \Omega_k(1 + z)^2. \tag{17}$$

This model has been thoroughly scrutinized from the observational point of view; indeed, its compatibility with the Cosmic Microwave Background Radiation (CMBR) peak location and amplitudes [28,29], with SNe Ia data [17,30] and gravitational lensing statistics [31,32] has been analyzed by various groups. The issue of structure formation [8,9,33] and its difficulties [34] have been recently addressed [35]. More recent analysis, based on the 194 SNe Ia data points from Ref. [23], has yielded interesting results in what concerns the allowed parameter space of the model [17]:

(1) Data favors $\alpha > 1$, although there is a strong degeneracy on α. At the 68% confidence level the minimal allowed values for α and A_s are 0.78 and 0.778, which rules out the ΛCDM model $\alpha = 0$ case. However, at the 95% confidence level it is found that there is no constraint on α.

(2) Dropping the assumption of flat prior, it is found that GCG is consistent with data for values of α sufficiently different from zero. Allowing for some small curvature, positive or negative, one finds that the GCG model is a more suitable description than the ΛCDM model.

These results are similar to the ones obtained in Refs. [14,15], where it is concluded that the supernova data of Ref. [23] favors "phantom"-like matter with an equation of state of the form $p = \omega\rho$ with $\omega < -1$.

In our present analysis, we have new results both with and without flat prior. For the flat case, the 68% and 95% confidence level contours are quite similar both with and

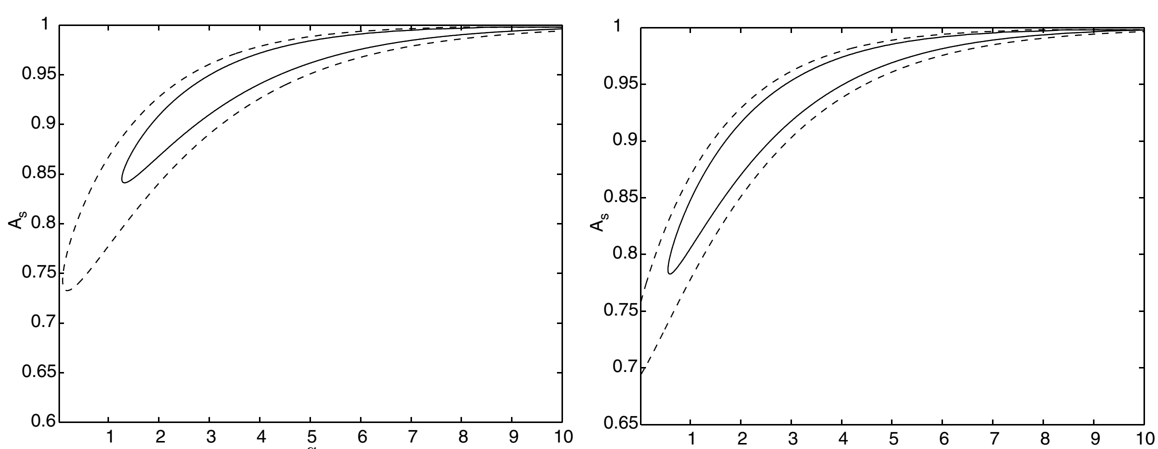

FIG. 5. Confidence contours in the and $A_s - \alpha$, parameter space for the flat GCG model. The solid and dashed lines represent the 68% and 95% confidence regions, respectively.

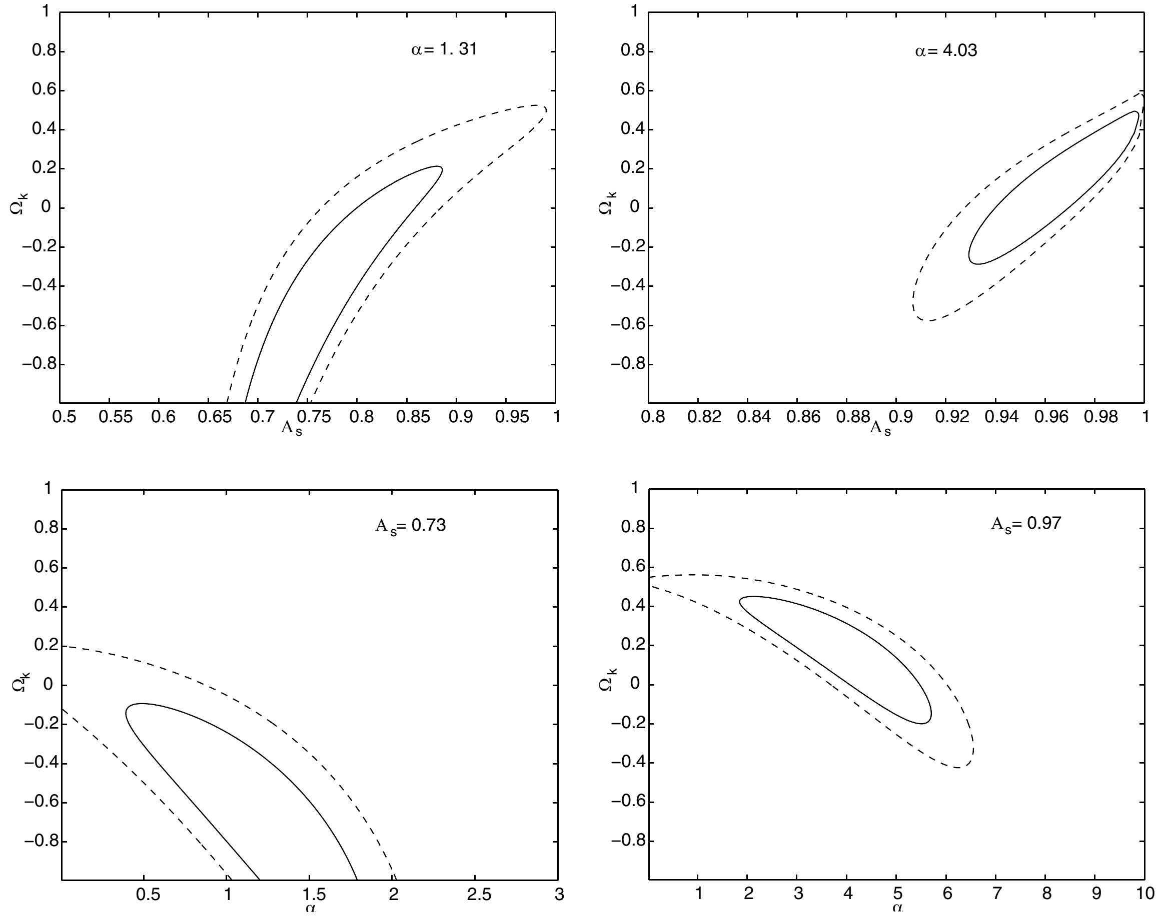

FIG. 6. Confidence contours in the $\Omega_k - A_s$ and $\Omega_k - \alpha$ parameter space for the nonflat GCG model. The solid and dashed lines represent the 68% and 95% confidence regions, respectively.

without HST data with that obtained by [17] as shown in Fig. 5. But still there is one interesting feature to note. It appears now that without the HST data, ΛCDM model ($\alpha = 0$) is ruled out even at 95% confidence level which was not the case in the previous analysis. But incorporating the HST data, again makes ΛCDM model consistent at 95% C.L although it is still ruled out at 68% C.L.

When we relax the condition of flat prior, one can observe some interesting features (See Fig. 6. Without the HST data, supernova data prefers a nonflat model, but the flat case is consistent both at 68% and 95% C.L if one chooses a value for α sufficiently different from zero. This means without flat prior, and without HST data, data prefers a curved model for GCG but the flat case is still consistent which is similar to the conclusion in [17].

But now if one includes the HST data, the best-fit model itself becomes a very close to flat case ($\Omega_k = 0.02$, Table II) which is a completely new feature. This shows that with the new HST data, the current gold sample of supernova data prefers a flat GCG model which is consistent with CMBR observation. It also shows that GCG is a better choice among the three possible choices of alternative models that we have considered here as far the gold sample of supernova data including those from HST measurements are concerned.

VI. DEGENERACY WITH XCDM MODEL

To illustrate the degeneracy between our models and the XCDM model, with constant equation of state $P/\rho = w_X$ and dark energy density $\Omega_X = 1 - \Omega_m$, let us consider the Taylor expansion of the luminosity distance as

$$d_L = \frac{c}{H_0}\left[z + \frac{(1-q_0)}{2} z^2 - \frac{1}{6}(1 - q_0 - 3q_0^2 + j_0) z^3 + \cdots \right], \tag{18}$$

where q_0 is the deceleration parameter, related with the second derivative of the scale-factor, and j_0 is the so-called statefinder or jerk parameter [36], related with the third derivative of the scale-factor. The subscript "0" means that quantities are evaluated at present. The jerk parameter is related with the deceleration parameter q_0 as

$$j_0 = q_0 + 2q_0^2 + \left.\frac{dq}{dz}\right|_0. \tag{19}$$

Notice that the jerk parameter is related to the geometry of the Universe (see Ref. [37], where it is shown that the measurement of the cubic correction to the Hubble law via high-redshift supernovae is the first cosmological measurement, after the CMBR, that probes directly the effects of spatial curvature). We have calculated q_0 and $\frac{dq}{dz}|_0$ for our models and obtained the results shown in Table III. We have considered only the flat case and, for simplicity, we study the DGP model instead of the more generic DT model; Ω_m is the only parameter of this model.

For low redshifts, it is sufficient to consider the first two terms in the series expansion of the luminosity distance, Eq. (18). From the expression of q_0 for the GCG, we can see that in this case the SNe Ia can only constrain A_s, as q_0 is independent of α. However for the Cardassian model the q_0 dependence is both on Ω_m and n, allowing low redshifts SNe Ia to put constraints in the model.

Moreover, in order to have degeneracy between the models we are analyzing and the XCDM model, the q_0 parameter of these models must be equal, $q_0^{\mathrm{XCDM}} = q_0^{\mathrm{Model}i}$, which results that:

$$w_X = (n-1)\frac{1-\Omega_m}{\Omega_X} \quad \text{for Cardassian model;} \tag{20}$$

$$w_X = -\frac{1-\Omega_m}{(1+\Omega_m)\Omega_X} \quad \text{for DGP model;} \tag{21}$$

$$w_X = -\frac{A_s}{\Omega_X} \quad \text{for GCG model.} \tag{22}$$

If one goes to higher redshifts, one also has to consider the higher order terms in the expansion of $d_L(z)$; hence, in this case also the jerk parameters have to be equal, which means that $\frac{dq}{dz}|_0$ have to be the same. We get that for Cardassian model

$$w_X = n - 1, \tag{23}$$

$$\Omega_X = 1 - \Omega_m, \tag{24}$$

meaning that the dynamical evolution of this model is equivalent to a dark energy model with the same matter density and a constant equation of state given by $w_{\mathrm{eff}} = n - 1$; the equivalent dark energy potential can be written as $V(\phi) = A[\sinh k(\phi/\sigma + C)]^{-\sigma}$ with $\sigma = -2 - 2/(n-1)$ [18] (see also Ref. [38]). We have seen that negative values of n are preferred which is consistent with the fact that phantom equation of state, $w_X < -1$, is favored by the data [14,15,17].

For DGP model one finds

$$w_X = \frac{\Omega_m^2 - 2\Omega_m - 1}{(1+\Omega_m)^2}, \tag{25}$$

$$\Omega_X = \frac{\Omega_m^2 - 1}{\Omega_m^2 - 2\Omega_m - 1}. \tag{26}$$

We see that for $\Omega_m < 0.6$ the equation of state is phantomlike and, as $\Omega_m \to 0$, $w_X \to -1$. We saw that the SNe Ia prefer $\Omega_m \sim 0.2$, consistent with the fact that a phantom equation of state is favored. Moreover, the amount of matter needed in a XCDM model to be equivalent to a given DGP model is larger, $\Omega_m^{\mathrm{XCDM}} = 1 - \Omega_X \geq \Omega_m$.

For the GCG model we find

$$w_X = -\alpha(1 - A_s) - 1, \tag{27}$$

$$\Omega_X = \frac{A_s}{1 + \alpha(1 - A_s)}, \tag{28}$$

We see that for any GCG model, the corresponding dark energy model equation of state has to be always phantom type [17], as $\alpha > 0$ and $0 < A_s < 1$. Nevertheless, for low redshift data, GCG is degenerate with all kinds of constant equation of state dark energy models, including the ΛCDM model, as can be inferred from Eq. (22).

TABLE III. Deceleration and jerk parameters for XCDM, Cardassian, DGP, and GCG models.

Model	q_0	$\frac{dq}{dz}\|_0$
XCDM	$\frac{1}{2} + \frac{3}{2} w_X \Omega_X$	$\frac{9}{2} w_X^2 \Omega_X (1 - \Omega_X)$
Cardassian	$\frac{1}{2} + \frac{3}{2}(n-1)(1-\Omega_m)$	$\frac{9}{2}(n-1)^2 \Omega_m (1-\Omega_m)$
DGP	$\frac{1}{2} + \frac{3}{2}\frac{\Omega_m - 1}{1+\Omega_m}$	$\frac{9\Omega_m(1-\Omega_m)}{(1+\Omega_m)^3}$
GCG	$\frac{3}{2}(1-A_s) - 1$	$\frac{9}{2} A_s (1-A_s)(1+\alpha)$

VII. DISCUSSION AND CONCLUSIONS

In this paper we have performed likelihood analysis of the latest type Ia supernova data for three distinct dark matter models. We have considered the Cardassian model, the modified gravity Dvali-Turner model, and the generalized Chaplygin gas model of unification of dark energy and dark matter. We find that for SNe Ia most recent data allows, in all cases, for nontrivial constraints on model parameters as summarized in Table II. We find that for all models relaxing the flatness condition implies that data favors then a considerable negative curvature for the gold without the HST data set. For the gold data set the resulting best-fit value for the curvature is positive (the GCG model is nearly flat in this case). For all models we have found, in what concerns the deceleration and jerk parameters, the conditions under which they are degenerate to the XCDM model. Thus, SNe Ia data clearly favors phantomlike equivalent equations of state.

Finally, in what concerns the gold sample of supernova data including those from HST measurements, our analysis reveals that the GCG flat model is the better choice among the three possible alternative models that we have considered in this paper.

ACKNOWLEDGMENTS

The work of N. M. C. S. and A. A. S was supported by Fundação para a Ciência e a Tecnologia (FCT, Portugal) under the Grant Nos. SFRH/BD/4797/2001 and SFRH/BPD/12365/2003, respectively.

[1] Supernova Search Team Collaboration, A. G. Riess *et al.*, Astron. J. **116**, 1009 (1998); Supernova Cosmology Project Collaboration, S. Perlmutter *et al.*, Astrophys. J. **517**, 565 (1999); C. L. Bennett *et al.*, Astrophys. J. Suppl. Ser. **148**, 1 (2003); D. N. Spergel *et al.*, Astrophys. J. Suppl. Ser. **148**, 175 (2003);SDSS Collaboration, M. Tegmark *et al.*, Phys. Rev. D **69**, 103501 (2004); SDSS Collaboration, M. Tegmark *et al.*, Astrophys. J. **606**, 702 (2004).

[2] M. Bronstein, Phys. Z. Sowjetunion **3**, 73 (1933); O. Bertolami, Nuovo Cimento Soc. Ital. Fis. B **93B**, 36 (1986); Fortschr. Phys. **34**, 829 (1986); K. Freese, F. C. Adams, J. A. Frieman, and E. Mottola, Nucl. Phys. **B287**, 797 (1987).

[3] B. Ratra and P. J. E. Peebles, Phys. Rev. D **37**, 3406 (1988); Astrophys. J. Lett. **325**, L17 (1988); C. Wetterich, Nucl. Phys. **B302**, 668 (1988); R. R. Caldwell, R. Dave, and P. J. Steinhardt, Phys. Rev. Lett. **80**, 1582 (1998); P. G. Ferreira and M. Joyce, Phys. Rev. D **58**, 023503 (1998); I. Zlatev, L. Wang, and P. J. Steinhardt, Phys. Rev. Lett. **82**, 986 (1999); P. Binétruy, Phys. Rev. D **60**, 063502 (1999); T. Barreiro, E. J. Copeland, and N. J. Nunes, Phys. Rev. D **61**, 127301 (2000); A. Albrecht and C. Skordis, Phys. Rev. Lett. **84**, 2076 (2000); M. C. Bento and O. Bertolami, Gen. Relativ. Gravit. **31**, 1461 (1999); M. C. Bento, O. Bertolami, and P. T. Silva, Phys. Lett. B **498**, 62 (2001); J. P. Uzan, Phys. Rev. D **59**, 123510 (1999); T. Chiba, Phys. Rev. D **60**, 083508 (1999); O. Bertolami and P. J. Martins, Phys. Rev. D **61**, 064007 (2000); N. Banerjee and D. Pavón, Classical Quantum Gravity **18**, 593 (2001); A. A. Sen, S. Sen, and S. Sethi, Phys. Rev. D **63**, 107501 (2001); A. A. Sen and S. Sen, Mod. Phys. Lett. A **16**, 1303 (2001).

[4] Y. Fujii, Phys. Rev. D **61**, 023504 (2000); A. Masiero, M. Pietroni, and F. Rosati, Phys. Rev. D **61**, 023504 (2000); M.C. Bento, O. Bertolami, and N. C. Santos, Phys. Rev. D **65**, 067301 (2002); D. Blais and D. Polarski, Phys. Rev. D **70**, 084008 (2004).

[5] C. Armendariz-Picon, T. Damour, and V. Mukhanov, Phys. Lett. B **458**, 209 (1999); T. Chiba, T. Okabe, and M. Yamaguchi, Phys. Rev. D **62**, 023511 (2000); C. Armendariz-Picon, V. Mukhanov, and P. J. Steinhardt, Phys. Rev. D **63**, 103510 (2001); L. P. Chimento, Phys. Rev. D **69**, 123517 (2004); P. F. Gonzalez-Diaz, Phys. Lett. B **586**, 1 (2004); R. J. Scherrer, Phys. Rev. Lett. **93**, 011301 (2004); J. M. Aguirregabiria, L. P. Chimento, and R. Lazkoz, Phys. Rev. D **70**, 023509 (2004).

[6] R. R. Caldwell, Phys. Lett. B **545**, 23 (2002); S. M. Carroll, M. Hoffman, and M. Trodden, Phys. Rev. D **68**, 023509 (2003); G. W. Gibbons, hep-th/0302199; R. R. Caldwell, M. Kamionkowski, and N. N. Weinberg, Phys. Rev. Lett. **91**, 071301 (2003); A. E. Schulz and M. J. White, Phys. Rev. D **64**, 043514 (2001); S. Nojiri and S. D. Odintsov, Phys. Lett. B **562**, 147 (2003); P. Singh, M. Sami, and N. Dadhich, Phys. Rev. D **68**, 023522 (2003); M. P. Dabrowski, T. Stachowiak, and M. Szydlowski, Phys. Rev. D **68**, 103519 (2003); J. G. Hao and X. z. Li, Phys. Rev. D **70**, 043529 (2004); H. Stefancic, Phys. Lett. B **586**, 5 (2004); J. M. Cline, S. y. Jeon, and G. D. Moore, Phys. Rev. D **70**, 043543 (2004); M. G. Brown, K. Freese, and W. H. Kinney, astro-ph/0405353; V. K. Onemli and R. P. Woodard, Phys. Rev. D **70**, 107301 (2004); Classical Quantum Gravity **19**, 4607 (2002); A. Vikman, Phys. Rev. D **71**, 023515 (2005); S. Nesseris and L. Perivolaropoulos, Phys. Rev. D **70**, 123529 (2004); E. Babichev, V. Dokuchaev, and Yu. Eroshenko, Classical Quantum Gravity **22**, 143 (2005).

[7] A. Y. Kamenshchik, U. Moschella, and V. Pasquier, Phys. Lett. B **511**, 265 (2001).

[8] N. Bilic, G. B. Tupper, and R. D. Viollier, Phys. Lett. B **535**, 17 (2002).

[9] M. C. Bento, O. Bertolami, and A. A. Sen, Phys. Rev. D **66**, 043507 (2002).

[10] G. Dvali and M. S. Turner, astro-ph/0301510.

[11] G. R. Dvali, G. Gabadadze, and M. Porrati, Phys. Lett. B **485**, 208 (2000).

[12] C. Deffayet, G. R. Dvali, G. Gabadadze, and A. Lue, Phys. Rev. D **64**, 104002 (2001); C. Deffayet, Phys. Lett. B **502**, 199 (2001).

[13] K. Freese and M. Lewis, Phys. Lett. B **540**, 1 (2002).

[14] T. R. Choudhury and T. Padmanabhan, Astron. Astrophys. **429**, 807 (2005).

[15] U. Alam, V. Sahni, T. D. Saini, and A. A. Starobinsky, Mon. Not. R. Astron. Soc. **354**, 275 (2004).

[16] S. Nesseris and L. Perivolaropoulos, Phys. Rev. D **70**, 043531 (2004).

[17] O. Bertolami, A. A. Sen, S. Sen, and P. T. Silva, Mon. Not. R. Astron. Soc. **353**, 329 (2004).

[18] Y. G. Gong and C. K. Duan, Mon. Not. R. Astron. Soc. **352**, 847 (2004).

[19] Z. H. Zhu, M. K. Fujimoto, and X. T. He, Astrophys. J. **603**, 365 (2004).

[20] O. Elgaroy and T. Multamaki, astro-ph/0404402 [Mon. Not. Roy. Astron. Soc. (to be published)].

[21] A. A. Sen and S. Sen, Phys. Rev. D **68**, 023513 (2003).

[22] Supernova Search Team Collaboration, A. G. Riess *et al.*, Astrophys. J. **607**, 665 (2004).

[23] Supernova Search Team Collaboration, J. L. Tonry *et al.*, Astrophys. J. **594**, 1 (2003).

[24] B. J. Barris *et al.*, Astrophys. J. **602**, 571 (2004).

[25] http://cernlib.web.cern.ch/cernlib/download/ / 2004_source/tar/minuit32_src.tar.gz

[26] D. J. H. Chung and K. Freese, Phys. Rev. D **61**, 023511 (2000).

[27] P. Gondolo and K. Freese, Phys. Rev. D **68**, 063509 (2003).

[28] M. C. Bento, O. Bertolami, and A. A. Sen, Phys. Rev. D **67**, 063003 (2003); Phys. Lett. B **575**, 172 (2003); Gen. Relativ. Gravit. **35**, 2063 (2003).

[29] D. Caturan and F. Finelli, Phys. Rev. D **68**, 103501 (2003); L. Amendola, F. Finelli, C. Burigana, and D. Caturan, J. Cosmol. Astropart. Phys. 07 (2003) 005.

[30] J. C. Fabris, S. B. V. Gonçalves, and P. E. de Souza, astro-ph/0207430;A. Dev, J. S. Alcaniz, and D. Jain, Phys. Rev. D **67**, 023515 (2003); V. Gorini, A. Kamenshchik, and U. Moschella, Phys. Rev. D **67**, 063509 (2003); M. Makler, S. Q. de Oliveira, and I. Waga, Phys. Lett. B **555**, 1 (2003); J. S. Alcaniz, D. Jain, and A. Dev, Phys. Rev. D **67**, 043514 (2003).

[31] P. T. Silva and O. Bertolami, Astrophys. J. **599**, 829 (2003).

[32] A. Dev, D. Jain, D. D. Upadhyaya, and J. S. Alcaniz, Astron. Astrophys. **417**, 847 (2004).

[33] J. C. Fabris, S. B. V. Gonçalves, and P. E. de Souza, Gen. Relativ. Gravit. **34**, 53 (2002).

[34] H. Sandvik, M. Tegmark, M. Zaldarriaga, and I. Waga, Phys. Rev. D **69**, 123524 (2004).

[35] M. C. Bento, O. Bertolami, and A. A. Sen, Phys. Rev. D**70**, 083519 (2004).

[36] U. Alam, V. Sahni, T. D.Saini, and A. A. Starobinsky, Mon. Not. R. Astron. Soc. **344**, 1057 (2003); V. Sahni, T. D. Saini, A. A. Starobinsky, and U. Alam, JETP Lett. **77**, 201 (2003); M. Visser, Classical Quantum Gravity **21**, 2603 (2004); M. P. Dabrowski and T. Stachowiak, hep-th/0411199.

[37] R. R. Caldwell and M. Kamionkowsky, astro-ph/0403003.

[38] V. Sahni and A. A. Starobinsky, Int. J. Mod. Phys. D **9**, 373 (2000).